

The Standard siren tests of viable $f(R)$ cosmologies

Yi Zhang^{a,1}, Xuanjun Niu¹, Xianfu Su², Dong-Ze He¹

¹School of Electronic Science and Engineering, Chongqing University of Posts and Telecommunications, Chongqing 400065, China
²Zhijin No.9 Senior High School, Guizhou 552100, China

Received: date / Accepted: date

Abstract We constrain the Hu-Sawicki and Starobinsky $f(R)$ gravity models utilizing current electromagnetic (PP+CC, Planck and DESI2) datasets and simulate standard siren catalogs based on the resulting best-fit parameters. We demonstrate that the simulated SS data provide complementary sensitivity to the modified gravitational wave propagation friction term, thereby enhancing the discriminating power between $f(R)$ gravity and the Λ CDM model. However, we note that standard sirens do not offer a viable resolution to the Hubble tension in this analysis, as the inferred constraints are predominantly driven by the fiducial cosmologies adopted in the simulations. Regarding the specific models, we find that for the Hu-Sawicki scenario, several data combinations favor $F_{RR0} < 0$, implying potential theoretical instabilities. And, for the Starobinsky model, while EM-only constraints are nearly symmetric between the two parameter branches ($b < 0$ and $b > 0$), the inclusion of SS constraints introduces mild asymmetries, revealing the sensitivity of SS observables to the curvature dependence of the theory. Future truly independent standard siren observations would be crucial for a definitive assessment of $f(R)$ gravity as an alternative to Λ CDM.

1 Introduction

Recent baryon acoustic oscillation (BAO) measurements from the Dark Energy Spectroscopic Instrument (DESI) [1, 2], especially when combined with cosmic microwave background (CMB) and Type Ia supernova (SNe Ia) observations, suggest a mild preference for departures from a pure cosmological constant and therefore motivate tests of a dynamical dark-energy sector. At the same time, despite extensive theoretical efforts, many cosmological models remain challenged by the Hubble tension in electromagnetic (EM)

data, commonly defined as a $> 5\sigma$ discrepancy between local distance ladder and CMB inferred determinations of the Hubble constant H_0 [3–8]. Such tensions may arise from unaccounted systematics or, more intriguingly, from physics beyond the standard Λ CDM framework. These considerations provide strong motivation to test modified gravity scenarios as alternatives to Λ CDM model.

Among modified gravity theories, $f(R)$ gravity offers a natural and minimal extension of general relativity (GR) that can account for late-time cosmic acceleration without invoking a fundamental cosmological constant, while still admitting a continuous Λ CDM limit. Phenomenologically, this can be interpreted as an effective dark energy equation of state $w_{\text{eff}}(z)$ that deviates from -1 and may evolve with redshift z . However, when constrained solely by EM probes of the background expansion, most viable $f(R)$ models are notoriously difficult to distinguish from Λ CDM [9–24]. This motivates the use of complementary observables with enhanced sensitivity to modified gravity effects. A key question is therefore whether $f(R)$ gravity can provide a viable alternative to Λ CDM when confronted with forthcoming standard siren (SS) tests.

Gravitational waves (GWs), a cornerstone prediction of GR, provide such an independent probe. Since the first detection of the binary black hole merger GW150914, hundreds of compact-binary coalescences have been observed [25–30]. In particular, standard sirens yield a direct measurement of the luminosity distance D_L^{SS} without relying on the cosmic distance ladder. In modified gravity, the SS luminosity distance can differ from its EM counterpart due to an effective friction term in GW propagation, providing a powerful discriminator between modified gravity and Λ CDM [31, 32]. Although the current number of SS events is still limited, future detectors such as the Einstein Telescope (ET) are expected to observe large samples of binary neutron star mergers (including lensed events), enabling high-precision

^ae-mail: zhangyia@cqupt.edu.cn

tests of GR and Λ CDM [33, 34]. Following the simulation frameworks of Refs. [35–40], we will generate mock ET standard siren catalogs to assess whether SS observations can break the degeneracy between $f(R)$ gravity and Λ CDM here.

In this work we focus on two representative and widely studied $f(R)$ models: the Hu-Sawicki and Starobinsky models [41, 42], which satisfy standard viability conditions and recover Λ CDM in an appropriate limit. Motivated by the bimodal posteriors discussed in Ref. [12], we further split the Starobinsky model into two branches with $b > 0$ and $b < 0$. Since EM data (SNe Ia, BAO, and CMB) alone do not provide decisive evidence for dynamical dark energy, we use the EM best fitted results as fiducial inputs for our SS simulations in order to isolate and quantify the additional impact of standard sirens.

This paper is organized as follows. In Sec. 2 we introduce the Hu-Sawicki and Starobinsky models. In Sec. 3 we describe the EM and standard siren datasets used in the analysis. The cosmological constraints and discussion are presented in Sec. 4. Finally, we summarize our conclusions in Sec. 5.

2 The $f(R)$ models

In the metric formalism, the Einstein-Hilbert action is generalized by replacing the Ricci scalar R with a generic function $f(R)$. A general $f(R)$ theory minimally coupled to matter is described by

$$S = \int d^4x \sqrt{-g} \left[\frac{f(R)}{16\pi G} + \mathcal{L}_m \right], \quad (1)$$

where \mathcal{L}_m denotes the Lagrangian of the non-gravitational matter sector, including dark matter.¹ The function $f(R)$ encodes deviations from general relativity (GR) and may account for the late-time cosmic acceleration. It is convenient to decompose

$$f(R) = R + F(R), \quad (2)$$

so that $F(R)$ measures the departure from GR. Varying the action with respect to the metric yields the modified Einstein equations. For a spatially flat Friedmann-Robertson-Walker (FRW) background, the Ricci scalar is

$$R = 12H^2 + 6\dot{H}, \quad (3)$$

and the modified Friedmann equations can be written as

$$3f_R H^2 - \frac{Rf_R - f(R)}{2} + 3Hf_{RR}\dot{R} = 8\pi G \rho_m, \quad (4)$$

$$-2f_R\dot{H} = 8\pi G \rho_m + \ddot{f}_R - H\dot{f}_R, \quad (5)$$

where overdots denote derivatives with respect to cosmic time t , ρ_m is the matter energy density, and $f_R \equiv df/dR$, $f_{RR} \equiv d^2f/dR^2$.

¹We neglect radiation, which is subdominant at late times.

The coupled system in Eqs. (4) and (5) typically does not admit closed-form solutions. In practice, viable models such as the Hu-Sawicki and Starobinsky forms are constructed to smoothly approach Λ CDM in an appropriate limit. Their functional form can be cast as

$$f(R) = R - 2\Lambda y(R, b), \quad (6)$$

where Λ is an effective cosmological constant and $y(R, b)$ parametrizes the deviations from Λ CDM via a dimensionless parameter b . For $b > 0$, one has $\lim_{b \rightarrow 0} f(R) = R - 2\Lambda$ and $\lim_{b \rightarrow \infty} f(R) = R$. In particular, as $F_R \rightarrow 0$ and $F_{RR} \rightarrow 0$ the theory continuously reduces to Λ CDM. Although originally proposed as cosmological constant free models, both the Hu-Sawicki and Starobinsky constructions effectively contain a Λ term in the relevant limit [41, 42].

Defining the normalized Hubble rate $E(a) \equiv H/H_0$, an effective dark-energy equation of state can be expressed as

$$w_{\text{eff}}(a) = \frac{-1 - \frac{2a}{3} \frac{d \ln E}{da}}{1 - \Omega_m(a)}, \quad (7)$$

where $\Omega_m(a) = \Omega_{m0}a^{-3}/E^2(a)$. In the Λ CDM limit, $w_{\text{eff}} = -1$.

Following Basilakos et al. [12], we adopt an efficient approximation scheme based on expanding the Hubble rate around the Λ CDM solution, which avoids expensive numerical integrations and has been widely used [9–11, 43]. Rewriting Eq. (4) in terms of the e-folding number $N = \ln a$, we obtain

$$-f_R H^2(N) + \Omega_{m0} e^{-3N} + \frac{1}{6} (Rf_R - f) = f_{RR} H^2(N) R'(N) \quad (8)$$

where the prime “ $'$ ” denotes derivative with respect to N . To quantify deviations from Λ CDM we expand around $b = 0$; keeping the first two nonzero terms reproduces the numerical solution to better than 0.001% for $b \in [0.001, 0.5]$. Specifically,

$$H^2(N) = H_\Lambda^2(N) + \sum_{i=1}^M b^i \delta H_i^2(N), \quad (9)$$

$$H_\Lambda^2(N) = \Omega_{m0} e^{-3N} + (1 - \Omega_{m0}), \quad (10)$$

where M denotes the truncation order.

The dynamical properties of $f(R)$ models can be conveniently characterized by two dimensionless variables [17, 44],

$$r \equiv -\frac{Rf_R}{f(R)} = -\frac{R(1+F_R)}{f(R)}, \quad (11)$$

$$m \equiv \frac{Rf_{RR}}{f_R} = \frac{RF_{RR}}{1+F_R}. \quad (12)$$

Here, $f_R = 1 + F_R$ and $f_{RR} = F_{RR}$. The quantity f_R controls the effective gravitational coupling, $G_{\text{eff}} \propto f_R^{-1}$, whereas f_{RR} governs the dynamics of the additional scalar degree of freedom (the scalaron) and thus sets how rapidly deviations from

GR/ΛCDM can develop. The variable r measures the proximity to the ΛCDM limit, while the variable m quantifies the strength of the deviation; in many dynamical analyses $m < 0$ signals an instability [17]. Viable cosmologies correspond to trajectories in the (r, m) plane that pass close to the GR limit $(r, m) \simeq (-1, 0^+)$ during the radiation and matter eras and then approach a stable de Sitter fixed point near $r \simeq -2$ with $0 < m < 1$. Within this framework, departures from ΛCDM, for example $w_{\text{eff}}(z) \neq -1$ and its redshift evolution, can be interpreted as resulting from the evolution of the (r, m) variables (equivalently, from the curvature dependence encoded in $m(R)$).

2.1 The Hu-Sawicki model

Hu and Sawicki [41] proposed a viable $f(R)$ model of the form

$$F(R) = -\tilde{m}^2 \frac{c_1 (R/\tilde{m}^2)^n}{1 + c_2 (R/\tilde{m}^2)^n}, \quad (13)$$

where $\tilde{m}^2 = \Omega_{m0} H_0^2$, c_1 , c_2 , and n are free parameters. Equivalence principle tests typically require $n \gtrsim 0.9$ [18]; in this work we restrict to $n = 1$. For $n = 1$, the model can be rewritten as

$$F(R) = -\frac{2\Lambda}{1 + b\Lambda/R}, \quad (14)$$

where $b \equiv 2/c_1$ and $\Lambda = \tilde{m}^2 c_1 / (2c_2)$. The Hu-Sawicki model can be made arbitrarily close to ΛCDM by taking $b \rightarrow 0$. In this case, Eq. (6) yields

$$y_{\text{HS}}(R, b) = 1 - \frac{1}{1 + R/(b\Lambda)}. \quad (15)$$

For later use, the first two derivatives of Eq. (14) with respect to R are listed as

$$F_R = -\frac{2}{b(1 + R/(b\Lambda))^2}, \quad (16)$$

$$F_{RR} = \frac{4}{b^2 \Lambda (1 + R/(b\Lambda))^3}, \quad (17)$$

where F_R is an odd function, while F_{RR} is an even one.

Expanding the Hubble rate according to Eq. (9), we obtain

$$H_{\text{HS}}^2(N) = H_\Lambda^2(N) + b \delta H_1^2(N) + b^2 \delta H_2^2(N) + \dots, \quad (18)$$

where $\delta H_1^2(N)$ and $\delta H_2^2(N)$ are given in Ref. [12]. The leading departure from ΛCDM appears at $\mathcal{O}(b)$, i.e. this model is Λ-like in the small- b regime.

2.2 The Starobinsky model

The Starobinsky model [42] is defined by

$$F(R) = -c_1 \tilde{m}^2 \left[1 - (1 + R^2/\tilde{m}^4)^{-n} \right], \quad (19)$$

where $\tilde{m}^2 = \Omega_{m0} H_0^2$, and c_1 and n are free parameters. It has been argued that n should be an integer [19]; therefore we set $n = 1$ following Ref. [12]. For $n = 1$, the model can be written as

$$F(R) = -2\Lambda \frac{(R/(b\Lambda))^2}{1 + (R/(b\Lambda))^2}, \quad (20)$$

where $\Lambda = c_1 \tilde{m}^2 / 2$ and $b \equiv 2/c_1$. The model approaches ΛCDM in the limit $b \rightarrow 0$. The corresponding deviation function is

$$y_{\text{Star}}(R, b) = 1 - \frac{1}{1 + (R/(b\Lambda))^2}. \quad (21)$$

The first two derivatives of Eq. (20) are

$$F_R = -\frac{4R}{b^2 \Lambda \left[1 + (R/(b\Lambda))^2 \right]^2}, \quad (22)$$

$$F_{RR} = \frac{4}{b^2 \Lambda} \frac{3(R/(b\Lambda))^2 - 1}{\left[1 + (R/(b\Lambda))^2 \right]^3}, \quad (23)$$

which are two even functions. Stability requires $\tilde{m}^2 > 0$ for viable $f(R)$ models [45]. Expanding the Friedmann equation yields

$$H_{\text{Star}}^2(N) = H_\Lambda^2(N) + b^2 \delta H_2^2(N) + b^4 \delta H_4^2(N) + \dots, \quad (24)$$

where the leading correction appears at $\mathcal{O}(b^2)$. The explicit forms of $\delta H_2^2(N)$ and $\delta H_4^2(N)$ are given in Ref. [12] as well.

For the Starobinsky case, EM constraints on b may exhibit a bimodal structure [23]. To capture this feature, we impose the prior $b \neq 0$, which partitions the parameter space into two branches, $b < 0$ and $b > 0$, denoted as StarobinskyI and StarobinskyII (StarI and StarII for short).

3 Data and methodology

We constrain the parameters of the $f(R)$ models using a Markov Chain Monte Carlo (MCMC) analysis together with a maximum-likelihood estimation, implemented with `CosmoMC` [46]. In this section, we shall describe the electromagnetic datasets and the simulated standard siren data used in our analysis.

3.1 Electromagnetic datasets

We consider EM probes of the cosmic distance scale, including measurements of the Hubble parameter from cosmic chronometers (CC) [47, 48], Type Ia supernovae from the PantheonPlus (PP) compilation [49, 50], CMB distance priors from Planck [5], and BAO measurements from the DESI Data Release 2 (hereafter DESI2) [1, 2]. The PP and CC data mainly probe the late-time Universe, whereas CMB and BAO measurements are also sensitive to earlier epochs.

3.1.1 PantheonPlus + cosmic chronometers (PP+CC)

The PantheonPlus compilation provides 1701 distance modulus measurements from 18 independent surveys [49, 50] over the redshift range $0.00122 < z < 2.26137$. For PantheonPlus, we compute the likelihood using the full covariance matrix $\mathbf{C}_{\text{stat+sys}}$, which includes both statistical and systematic uncertainties.

The CC data estimate $H(z)$ from the differential ages of passively evolving galaxies. We adopt the compilation of 32 CC measurements listed in Table 1 of Ref. [48], including determinations based on galaxy age dating and BAO-related techniques [51–59].

Since the PP and CC datasets are mutually consistent [60], we combine them into a single dataset denoted PP+CC. The covariance matrices used in the likelihood follow Refs. [47, 56, 61]. The combined PP+CC dataset contains 1733 data points.

3.1.2 Planck distance prior

For CMB constraints, we use the distance priors derived from the Planck 2018 data release [5]. The distance prior approach [62–68] provides a compressed representation of the CMB information while retaining the key cosmological constraints relevant for background evolution. The priors are typically expressed in terms of the shift parameter R and the acoustic scale ℓ_a [62]. We adopt the data vector and covariance matrix from Ref. [68].

3.1.3 DESI2 BAO

Baryon acoustic oscillations provide a standard ruler for tracing the expansion history through features imprinted in the matter power spectrum. We use the DESI BAO release 2 (DESI2) [1, 2], which includes measurements from four classes of tracers: the bright galaxy sample (BGS) [69], luminous red galaxies (LRG) [70], emission line galaxies (ELG) [71], and quasars (QSO) [72].

DESI2 reports the transverse comoving distance D_M , the Hubble distance D_H , and the volume-averaged distance D_V , normalized by the sound horizon at the drag epoch r_d . We determine r_d using BBN information.² The measurements span seven redshift bins derived from over six million objects (see Table 1 of Refs. [1, 2]).

For LRG1, LRG2, LRG3+ELG1, ELG2, and Ly α QSO, DESI2 provides correlated pairs of $(D_M/r_d, D_H/r_d)$. Following Ref. [74], we construct the corresponding data vector and covariance matrix, using the correlation coefficients reported in Table 1 of Ref. [1].

²We adopt $\Omega_b h^2 = 0.022$ [73], where Ω_b is the baryon density parameter and $h \equiv H_0/(100 \text{ km s}^{-1} \text{ Mpc}^{-1})$.

3.2 Standard sirens

Gravitational waves emitted by compact binary coalescences can serve as the standard sirens to probe the cosmic expansion history [33, 34]. In particular, the luminosity distance D_L^{SS} can be inferred directly from the GW amplitude, without calibration from the cosmic distance ladder,

$$h_A = \frac{4}{D_L^{\text{SS}}} \left(\frac{GM_c}{c^2} \right)^{5/3} \left(\frac{\pi f_{\text{SS}}}{c} \right)^{2/3}, \quad (25)$$

where h_A is the GW amplitude, M_c is the chirp mass, and f_{SS} is the GW frequency.

In modified gravity theories, GW propagation generally follows [38, 40]

$$\bar{h}_A'' + 2\mathcal{H}[1 + \delta(\eta)]\bar{h}_A' + k^2\bar{h}_A = 0, \quad (26)$$

where the \bar{h}_A denotes the Fourier mode of the GW amplitude, prime “ $'$ ” denotes derivatives with respect to conformal time η , $\mathcal{H} \equiv a'/a$ is the conformal Hubble parameter, and δ is an extra friction term that vanishes in GR. Defining an effective scale factor \tilde{a} via

$$\frac{\tilde{a}'}{\tilde{a}} = \mathcal{H}[1 + \delta(z)], \quad (27)$$

and introducing $\chi_A \equiv \tilde{a}\bar{h}_A$, the propagation equation can be recast as [31]

$$\chi_A'' + \left(k^2 - \frac{\tilde{a}''}{\tilde{a}} \right) \chi_A = 0. \quad (28)$$

As a consequence, the SS and EM luminosity distances are related by

$$D_L^{\text{SS}}(z) = \exp \left[\int_0^z \frac{\delta(z')}{1+z'} dz' \right] D_L^{\text{EM}}(z). \quad (29)$$

In $f(R)$ gravity, the friction term is given by [75]

$$\delta = -\frac{\dot{R}F_{RR}}{2H(1+F_R)}, \quad (30)$$

which leads to the compact relation

$$\beta_T(z) \equiv \frac{D_L^{\text{SS}}(z)}{D_L^{\text{EM}}(z)} = \sqrt{\frac{1+F_{R0}}{1+F_R(z)}}. \quad (31)$$

By construction, $\beta_T(0) = 1$, and the departure of GW distances from EM distances is fully determined by the redshift evolution of F_R .

3.3 The method

We first constrain the cosmological models using the EM datasets PP+CC, Planck, and DESI2. The Markov chain Monte Carlo (MCMC) analysis is performed with *CosmoMC* [46]. For each EM dataset, the best-fit parameter values (corresponding to the minimum χ^2) are adopted as the fiducial cosmology to generate mock standard siren (SS) catalogs.

In our notation, the subscript “PP+CC/Planck/DESI2” indicates that the SS fiducial parameters are taken from the best-fit constraints obtained with the corresponding EM dataset. Following Refs. [35, 37, 38], we simulate 1000 SS events detectable by the Einstein Telescope (ET) over a 10-year observation period, including 500 binary neutron star (BNS) and 500 black hole-neutron star (BHNS) systems. The weak-lensing uncertainty is modeled as $\sigma_{\text{lens}} = 0.05z$.

For most simulations, we directly adopt the corresponding best-fit values as fiducial parameters. However, for the Hu-Sawicki model, the PP+CC best-fit values $(\Omega_{m0}, H_0, b) = (0.252, 78.65, 0.62)$ deviate substantially from the Λ CDM results. Directly using this parameter set as SS fiducials can lead to unphysical and/or unstable constraints. To avoid this issue, we instead use the Λ CDM-based SS_{PP+CC} mock catalog to constrain the Hu-Sawicki model, adopting the fiducial parameters

$$\Omega_{m0} = 0.348, H_0 = 72.99, b = 0, \quad (32)$$

which lie within the 2σ region of the PP+CC constraints for the Hu-Sawicki model. In particular, we denote this dataset as HS:SS _{Λ CDM:PP+CC}.

To quantify the Hubble tension, we use [76]

$$T_1(\theta) = \frac{|\theta(D_1) - \theta(D_2)|}{\sqrt{\sigma_\theta^2(D_1) + \sigma_\theta^2(D_2)}}, \quad (33)$$

where θ is the best fitted values of H_0 from different data sets; the first data set D_1 represents the constraining results of cosmological fitting; the second data set D_2 is the chosen baseline measurement, which is $H_0 = 73.17 \pm 0.86$ km/s/Mpc from the latest SH0ES Team [6–8]; and $\sigma_\theta(D_1)$ and $\sigma_\theta(D_2)$ represent the errors from D_1 and D_2 data sets respectively.

Finally, we assess model performance using the AIC and BIC criteria with the Λ CDM model as reference. And, for Gaussian errors, the difference between two models could be written as $\Delta AIC = \Delta\chi^2 + 2\Delta N$. Similar to the AIC, the difference denoted by BIC has the form $\Delta BIC = \Delta\chi^2 + \Delta N \ln m$, where ΔN is the number of additional parameters and m is the number of data points. The $\Delta AIC = 5$ ($\Delta BIC \geq 2$) and $\Delta AIC = 10$ ($\Delta BIC \geq 6$) are considered to be the positive and strong evidence against the weaker model respectively.

4 Discussion

The cosmological constraints are summarized in Tables 1 and 2. Generally, both the Hu-Sawicki and Starobinsky $f(R)$ models are consistent with the data and can account for the late-time accelerated expansion. For each dataset, the best-fit χ^2_{min} is comparable to the number of data points. In particular, the standard siren dataset yields $\chi^2_{\text{min}} \simeq 1000$, indicating good internal consistency of the simulations. As expected, the joint EM+SS analyses provide the tightest constraints for all models, with the EM data contributing the

dominant statistical weight. The impact of SS data on the Hubble tension is intrinsically dependent on the adopted simulations and fiducial cosmology, since the H_0 values inferred from SS analyses largely depend on the assumed fiducial model. Consequently, SS datasets constructed with similar fiducial assumptions tend to yield comparable levels of Hubble tension.

For the reference Λ CDM model, among the EM datasets, the Planck provides the tightest constraints on Ω_{m0} and H_0 . The 1σ confidence regions from PP+CC, DESI2, and Planck are clearly separated in the $\Omega_{m0} - H_0$ plane, in which the PP+CC constraint favors a substantially larger H_0 that is lying outside the 2σ regions inferred from Planck and DESI2. Within Λ CDM, SS datasets based on Planck or DESI2 fiducials may mildly reduce the inferred tension, whereas SS_{PP+CC} favors a higher H_0 because it assumes a larger fiducial Hubble constant. As a result, PP+CC+SS_{PP+CC} yields a tension of $\sim 0.34\sigma$, compared with 3.82σ and 6.06σ for the Planck and DESI2 related combinations, respectively, within the adopted simulations.

As shown in Fig. 2, for all considered $f(R)$ models Planck yields the overall tightest constraints, while PP+CC-related combinations prefer larger values of H_0 as Λ CDM model. Figs. 1 and 2 further show that our SS simulations are in good agreement with the PantheonPlus sample. For the Hu-Sawicki model, the SS luminosity-distance evolution follows a similar ordering to that in Λ CDM,

$$D_L^{\text{SS}_{\text{PP+CC}}} < D_L^{\text{SS}_{\text{DESI2}}} \lesssim D_L^{\text{SS}_{\text{Planck}}}.$$

In contrast, for the Starobinsky model (left panels of Fig. 2) the ordering becomes

$$D_L^{\text{SS}_{\text{PP+CC}}} < D_L^{\text{SS}_{\text{Planck}}} \lesssim D_L^{\text{SS}_{\text{DESI2}}}.$$

In most cases, the total constraining power remains dominated by EM observations. The constraints on the Hu-Sawicki parameter b are comparable to those in the Starobinsky model; however, for the derived quantity $w_{\text{eff}0}$ which is mainly controlled by b , the Hu-Sawicki model allows a substantially broader parameter range than the Starobinsky case.

Using the 1σ constraints from the EM+SS joint data, we show the redshift evolution of w_{eff} in Fig. 3, and of F_R , F_{RR} , r and m in Fig. 4. For all considered $f(R)$ models, the effective equation of state w_{eff} exhibits mild oscillatory behavior; F_R and r monotonically increase with redshift z , whereas F_{RR} and the deviation parameter m decrease with z . All models smoothly approach the Λ CDM limit around $z \simeq 2$, where $F_R \rightarrow 0$, $F_{RR} \rightarrow 0$, and $m \rightarrow 0$. According to Eq. (31), the increase of F_R implies $\beta_T \leq 1$, which leads to a smaller SS luminosity distance D_L^{SS} compared to its electromagnetic counterpart D_L^{EM} . And the Hu-Sawicki and Starobinsky models evolve in a similar region of the (r, m) phase space.

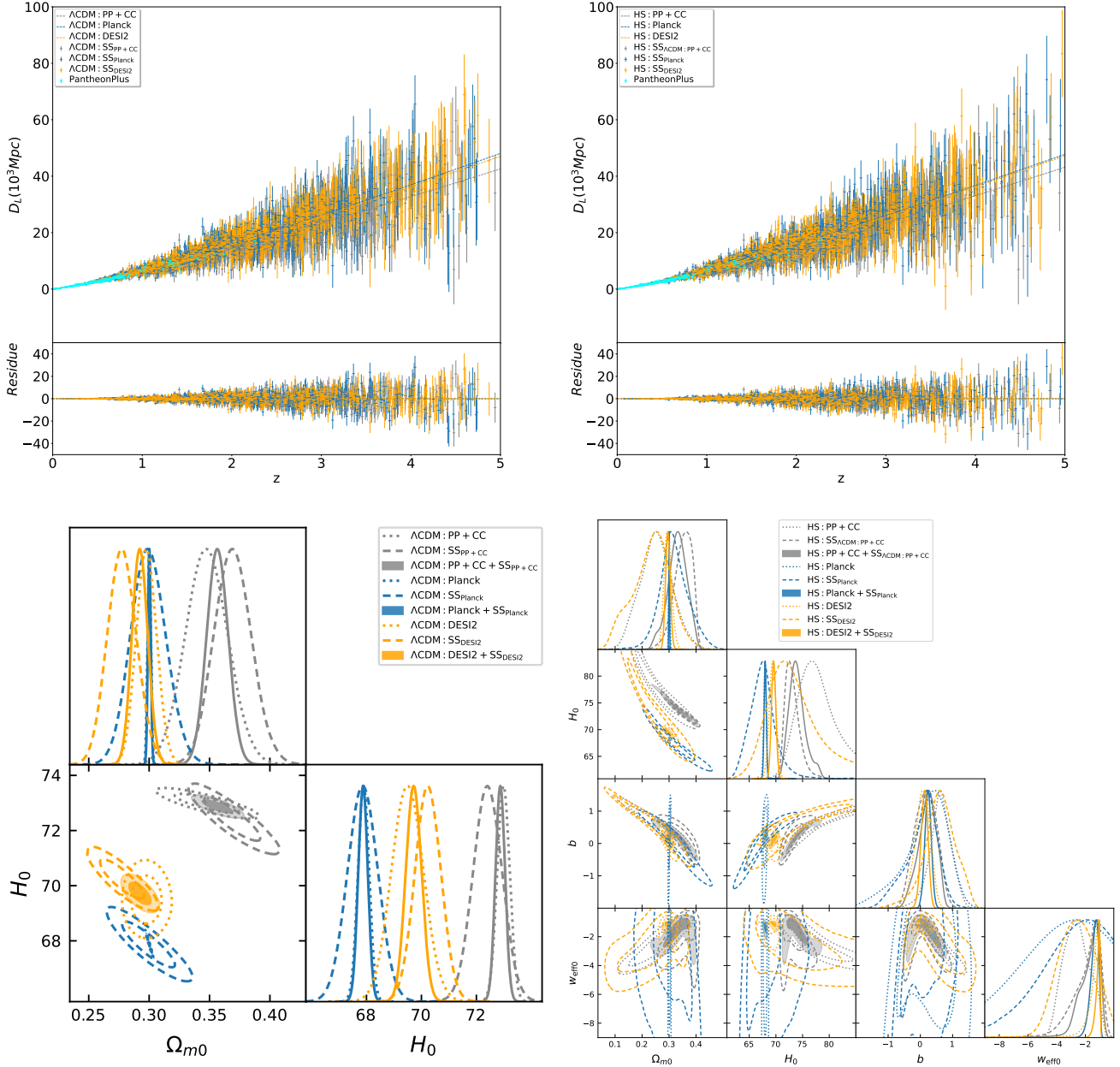


Fig. 1 *Left:* Comparison between luminosity-distance measurements from real and simulated datasets. The cyan points with error bars correspond to the PantheonPlus sample (real SNe Ia data). The gray/orange/blue points with error bars show the simulated standard siren datasets SS_{DESI2}/SS_{PP+CC}/SS_{Planck}, respectively. The gray/orange/blue solid curves represent the corresponding fiducial luminosity-distance relations used to generate the mock catalogs. *Right:* One and two dimensional marginalized posteriors (with 1σ and 2σ confidence regions) for the parameters of ΛCDM and the Hu-Sawicki model. The simulated datasets $\Lambda\text{CDM:SS}_{\text{DESI2}}$ / $\Lambda\text{CDM:SS}_{\text{PP+CC}}$ / $\Lambda\text{CDM:SS}_{\text{Planck}}$ are generated assuming ΛCDM with the EM best-fit fiducial parameters $(\Omega_{m0}^{\text{fid}}, H_0^{\text{fid}}) = (0.348, 72.99)/(0.298, 69.50)/(0.300, 67.89)$. For the Hu-Sawicki simulations, we adopt $(\Omega_{m0}^{\text{fid}}, H_0^{\text{fid}}, b^{\text{fid}}) = (0.348, 72.99, 0)$, $(0.296, 69.37, -0.06 \times 10^{-3})$, and $(0.301, 67.95, 0.15 \times 10^{-3})$ for HS:SS_{PP+CC}, HS:SS_{DESI2}, and HS:SS_{Planck}, respectively.

4.1 Discussion:Hu-Sawicki model

For the Hu-Sawicki model, all marginalized posterior probability density functions are approximately Gaussian as shown in Fig. 1. As reported in Table 1, the best-fit value $\chi^2_{\text{PP+CC}}$

is slightly smaller than that of the reference ΛCDM model. Taking ΛCDM as the baseline, we obtain $|\Delta\text{AIC}| < 5$ in all cases, implying that the AIC does not provide decisive model-selection evidence. By contrast, for the EM datasets we find $\Delta\text{BIC} = 4.7/3.0/3.4$ for PP+CC, Planck, and DESI2,

Table 1 Constraints on the primary parameters (Ω_{m0}, H_0, b) and the derived quantities $(w_{\text{eff0}}, \text{Hubble tension}, \chi^2)$ for ΛCDM , the Hu-Sawicki model and the Starobinsky model. For the standard siren simulations, the best fitted values inferred from the EM datasets (PP+CC/Planck/DESI2) are adopted as fiducial (baseline) parameters for the corresponding mock catalogs. In particular, $\text{HS:SS}_{\Lambda\text{CDM:PP+CC}}$ is generated using $(\Omega_{m0}, H_0, b) = (0.348, 72.99, 0)$ which is the best-fit parameters of the ΛCDM model. The Hubble tension is quantified with respect to the SH0ES determination $H_0 = 73.17 \pm 0.86 \text{ km s}^{-1} \text{ Mpc}^{-1}$ [6, 7], as described in Sec. 3.3.

Data	Ω_{m0}	$H_0(\text{km/s/Mpc})$	b	w_{eff0}	Hubble Tension	χ^2
$\Lambda\text{CDM:PP+CC}$	$0.348^{+0.017+0.033}_{-0.017-0.033}$	$72.99^{+0.21+0.42}_{-0.22-0.43}$	0	-1	0.20σ	1774.6
$\Lambda\text{CDM:SS}_{\text{PP+CC}}$	$0.369^{+0.015+0.03}_{-0.014-0.028}$	$72.41^{+0.50+0.99}_{-0.50-0.98}$	0	-1	0.76σ	981.8
$\Lambda\text{CDM:PP+CC+SS}_{\text{PP+CC}}$	$0.357^{+0.008+0.017}_{-0.009-0.017}$	$72.87^{+0.16+0.33}_{-0.16-0.32}$	0	-1	0.34σ	2755.6
$\Lambda\text{CDM: Planck}$	$0.300^{+0.001+0.003}_{-0.001-0.002}$	$67.89^{+0.20+0.38}_{-0.19-0.38}$	0	-1	5.99σ	2.8
$\Lambda\text{CDM:SS}_{\text{Planck}}$	$0.300^{+0.013+0.028}_{-0.014-0.027}$	$67.86^{+0.53+1.04}_{-0.52-1.03}$	0	-1	5.27σ	989.7
$\Lambda\text{CDM: Planck+SS}_{\text{Planck}}$	$0.300^{+0.001+0.002}_{-0.001-0.002}$	$67.87^{+0.17+0.33}_{-0.16-0.32}$	0	-1	6.06σ	990.6
$\Lambda\text{CDM:DESI2}$	$0.298^{+0.008+0.016}_{-0.008-0.016}$	$69.50^{+0.55+1.10}_{-0.55-1.10}$	0	-1	3.60σ	16.8
$\Lambda\text{CDM:SS}_{\text{DESI2}}$	$0.278^{+0.011+0.023}_{-0.012-0.023}$	$70.24^{+0.45+0.89}_{-0.45-0.89}$	0	-1	3.02σ	987.3
$\Lambda\text{CDM:DESI2+SS}_{\text{DESI2}}$	$0.292^{+0.007+0.013}_{-0.006-0.012}$	$69.72^{+0.28+0.54}_{-0.28-0.54}$	0	-1	3.82σ	1004.3
HS: PP+CC	$0.252^{+0.058+0.109}_{-0.056-0.108}$	$78.65^{+1.88+9.73}_{-5.34-7.06}$	$0.62^{+0.33+0.64}_{-0.29-0.95}$	$-2.628^{+1.608+1.644}_{-1.067-1.399}$	1.48σ	1771.8
HS:SS $_{\Lambda\text{CDM:PP+CC}}$	$0.351^{+0.045+0.049}_{-0.016-0.057}$	$73.16^{+0.63+2.71}_{-1.65-2.10}$	$0.17^{+0.35+0.58}_{-0.32-0.60}$	$-1.971^{+1.038+1.900}_{-0.296-1.921}$	0.01σ	982.3
HS:PP+CC+SS $_{\Lambda\text{CDM:PP+CC}}$	$0.331^{+0.036+0.069}_{-0.031-0.359}$	$74.04^{+1.00+3.93}_{-1.74-3.04}$	$0.21^{+0.32+0.47}_{-0.21-0.53}$	$-1.743^{+0.799+0.872}_{-0.265-1.220}$	0.54σ	2756.0
HS: Planck	$0.301^{+0.002+0.004}_{-0.002-0.004}$	$67.95^{+0.22+0.44}_{-0.22-0.44}$	$0.15^{+0.80+1.09}_{-0.37-1.45}$	$-5.584^{+4.778+5.075}_{-1.554-17.189}$	5.88σ	4.7
HS:SS $_{\text{Planck}}$	$0.319^{+0.044+0.108}_{-0.052-0.098}$	$67.60^{+1.71+4.45}_{-2.51-4.67}$	$0.04^{+0.57+0.77}_{-0.32-1.08}$	$-4.471^{+3.729+4.318}_{-1.804-17.575}$	2.44σ	987.4
HS: Planck+SS $_{\text{Planck}}$	$0.300^{+0.002+0.003}_{-0.001-0.002}$	$67.99^{+0.17+0.35}_{-0.19-0.36}$	$0.24^{+0.09+0.18}_{-0.10-0.19}$	$-1.383^{+0.335+0.412}_{-0.140-0.530}$	5.90σ	992.5
HS:DESI2	$0.296^{+0.012+0.028}_{-0.015-0.025}$	$69.37^{+0.62+1.21}_{-0.60-1.26}$	$0.06^{+0.26+0.42}_{-0.19-0.45}$	$-1.381^{+0.410+0.430}_{-0.027-0.982}$	3.60σ	17.7
HS:SS $_{\text{DESI2}}$	$0.235^{+0.077+0.109}_{-0.054-0.142}$	$75.06^{+1.69+16.43}_{-7.27-9.45}$	$0.60^{+0.47+0.73}_{-0.43-0.88}$	$-2.845^{+1.429+1.890}_{-0.920-1.358}$	0.41σ	984.9
HS:DESI2+SS $_{\text{DESI2}}$	$0.296^{+0.008+0.016}_{-0.008-0.016}$	$69.57^{+0.40+0.80}_{-0.39-0.79}$	$0.13^{+0.11+0.19}_{-0.10-0.22}$	$-1.152^{+0.164+0.175}_{-0.045-0.332}$	3.80σ	1002.0
StarI:PP+CC	$0.293^{+0.045+0.075}_{-0.029-0.083}$	$73.05^{+0.49+3.01}_{-0.92-1.82}$	$-1.05^{+0.13+1.05}_{-0.28-0.33}$	$-0.837^{+0.057+0.100}_{-0.044-0.161}$	0.11σ	1770.2
StarII:PP+CC	$0.293^{+0.045+0.076}_{-0.029-0.083}$	$73.08^{+0.47+3.36}_{-0.95-1.85}$	$1.05^{+0.29+0.34}_{-0.13-1.05}$	$-0.837^{+0.056+0.100}_{-0.044-0.161}$	0.08σ	1770.2
StarI:SS $_{\text{PP+CC}}$	$0.306^{+0.014+0.084}_{-0.044-0.056}$	$71.80^{+3.46+3.57}_{-1.13-5.81}$	$-1.17^{+0.14+1.17}_{-0.47-0.45}$	$-0.723^{+0.059+0.483}_{-0.265-0.299}$	0.55σ	983.6
StarII:SS $_{\text{PP+CC}}$	$0.306^{+0.019+0.066}_{-0.031-0.051}$	$72.55^{+2.61+3.27}_{-1.11-4.50}$	$1.00^{+0.46+0.46}_{-0.17-1.00}$	$-0.803^{+0.063+0.314}_{-0.184-0.227}$	0.30σ	988.6
StarI:PP+CC+SS $_{\text{PP+CC}}$	$0.297^{+0.013+0.028}_{-0.015-0.030}$	$72.48^{+0.67+1.06}_{-0.37-1.16}$	$-1.16^{+0.08+0.24}_{-0.13-0.22}$	$-0.795^{+0.036+0.090}_{-0.041-0.086}$	0.69σ	2752.6
StarII:PP+CC+SS $_{\text{PP+CC}}$	$0.304^{+0.013+0.027}_{-0.013-0.028}$	$72.47^{+0.60+0.94}_{-0.37-1.05}$	$1.10^{+0.15+0.19}_{-0.09-1.10}$	$-0.810^{+0.044+0.090}_{-0.040-0.100}$	0.71σ	2756.1
StarI: Planck	$0.301^{+0.002+0.004}_{-0.002-0.003}$	$67.97^{+0.21+0.42}_{-0.21-0.40}$	$-0.53^{+0.30+0.53}_{-0.34-0.45}$	$-0.950^{+0.019+0.097}_{-0.053-0.057}$	5.87σ	2.5
StarII: Planck	$0.301^{+0.002+0.004}_{-0.002-0.004}$	$67.97^{+0.21+0.41}_{-0.21-0.40}$	$0.53^{+0.16+0.45}_{-0.53-0.53}$	$-0.950^{+0.019+0.097}_{-0.054-0.057}$	5.87σ	2.5
StarI:SS $_{\text{Planck}}$	$0.335^{+0.012+0.081}_{-0.034-0.052}$	$65.74^{+2.37+2.68}_{-0.28-5.16}$	$-0.73^{+0.73+0.73}_{-0.28-0.75}$	$-0.839^{+0.046+0.653}_{-0.205-0.238}$	4.70σ	984.4
StarII:SS $_{\text{Planck}}$	$0.318^{+0.003+0.056}_{-0.031-0.054}$	$66.99^{+1.89+2.72}_{-0.88-8.60}$	$0.54^{+0.21+1.05}_{-0.54-0.54}$	$-0.898^{+0.006+0.877}_{-0.139-0.196}$	4.73σ	988.8
StarI: Planck+SS $_{\text{Planck}}$	$0.301^{+0.001+0.003}_{-0.001-0.003}$	$67.87^{+0.17+0.33}_{-0.17-0.34}$	$-0.40^{+0.40+0.40}_{-0.12-0.29}$	$-0.974^{+0.011+0.041}_{-0.027-0.030}$	6.05σ	987.1
StarII: Planck+SS $_{\text{Planck}}$	$0.301^{+0.001+0.003}_{-0.002-0.003}$	$68.00^{+0.16+0.33}_{-0.18-0.36}$	$0.51^{+0.26+0.27}_{-0.12-0.51}$	$-0.960^{+0.019+0.049}_{-0.036-0.043}$	5.90σ	989.7
StarI:DESI2	$0.325^{+0.018+0.042}_{-0.030-0.039}$	$64.32^{+5.16+5.55}_{-4.09-4.73}$	$-0.99^{+0.11+0.99}_{-0.43-0.40}$	$-0.778^{+0.135+0.271}_{-0.215-0.247}$	1.88σ	14.4
StarII:DESI2	$0.325^{+0.018+0.042}_{-0.030-0.039}$	$64.32^{+5.16+5.55}_{-4.09-4.74}$	$0.99^{+0.43+0.40}_{-0.12-0.99}$	$-0.778^{+0.134+0.273}_{-0.213-0.248}$	1.88σ	14.4
StarI:SS $_{\text{DESI2}}$	$0.335^{+0.016+0.030}_{-0.010-0.028}$	$64.88^{+0.28+0.64}_{-0.34-1.02}$	$-0.51^{+0.51+0.51}_{-0.19-0.52}$	$-0.938^{+0.024+0.132}_{-0.069-0.072}$	9.07σ	983.2
StarII:SS $_{\text{DESI2}}$	$0.358^{+0.022+0.053}_{-0.030-0.046}$	$62.80^{+2.05+2.62}_{-1.24-3.06}$	$0.96^{+0.43+0.42}_{-0.14-0.96}$	$-0.738^{+0.108+0.367}_{-0.252-0.291}$	5.59σ	987.4
StarI:DESI2+SS $_{\text{DESI2}}$	$0.334^{+0.014+0.033}_{-0.019-0.031}$	$63.75^{+1.23+2.05}_{-1.02-2.32}$	$-1.10^{+0.10+0.23}_{-0.13-0.23}$	$-0.753^{+0.058+0.183}_{-0.101-0.150}$	6.65σ	1000.2
StarII:DESI2+SS $_{\text{DESI2}}$	$0.340^{+0.015+0.032}_{-0.017-0.031}$	$62.72^{+1.01+2.09}_{-1.07-2.05}$	$1.19^{+0.11+0.19}_{-0.08-0.19}$	$-0.696^{+0.068+0.196}_{-0.098-0.151}$	7.74σ	1000.5

respectively, which constitutes positive evidence against ΛCDM of the adopted simulations, this can be interpreted as strong evidence against ΛCDM . Moreover, since the PP+CC-based SS simulations adopt ΛCDM evidence against ΛCDM , fiducial parameters (see Sec. 3.3), they also allow a meaningful assessment of model-selection evidence within the simulated setup. Because the corresponding SS constraints prefer values of Ω_{m0} that differ from those favored by Planck and DESI2, the $\text{SS}_{\Lambda\text{CDM:PP+CC}}$ related combinations yield even larger BIC differences, $\Delta\text{BIC} = 7.4/8.3$. In the context

The constraints inferred from the SS simulations exhibit nearly parallel confidence contours. Among them, SS_{DESI2} produces the widest constraints. For instance, in the $\Omega_{m0} - H_0$ plane the relative constraining power satisfies $\text{SS}_{\Lambda\text{CDM:PP+CC}} < \text{SS}_{\text{Planck}} < \text{SS}_{\text{DESI2}}$. In particular, PP+CC-related combinations yield systematically smaller Hubble tensions than the Planck and DESI2 re-

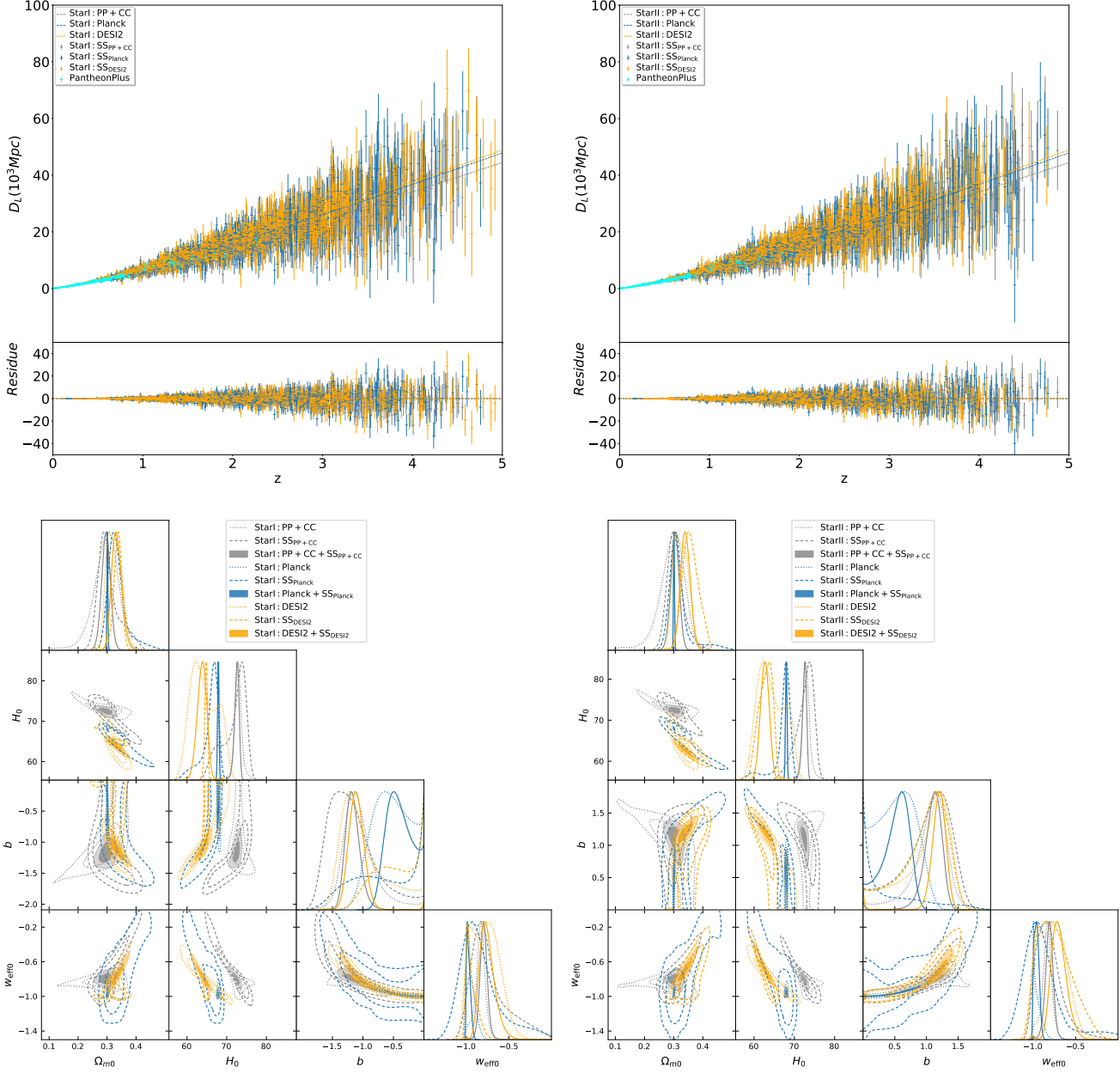


Fig. 2 Same as Fig. 1, but for the StarobinskyI ($b < 0$) and StarobinskyII ($b > 0$) models. For the corresponding standard siren simulations, the EM best-fit values from PP+CC/Planck/DESI2 are adopted as fiducial (baseline) parameters. Specifically, the mock catalogs StarI:SS_{PP+CC}, StarI:SS_{DESI2}, and StarI:SS_{Planck} are generated using $(\Omega_{m0}^{\text{fid}}, H_0^{\text{fid}}, b^{\text{fid}}) = (0.293, 73.05, -1.05 \times 10^{-3})$, $(0.325, 64.32, -0.99 \times 10^{-3})$, and $(0.301, 67.97, -0.53 \times 10^{-3})$, respectively. Likewise, the mock catalogs StarII:SS_{PP+CC}, StarII:SS_{DESI2}, and StarII:SS_{Planck} are generated using $(\Omega_{m0}^{\text{fid}}, H_0^{\text{fid}}, b^{\text{fid}}) = (0.293, 73.08, 1.05 \times 10^{-3})$, $(0.325, 64.32, 0.99 \times 10^{-3})$, and $(0.301, 67.97, 0.53 \times 10^{-3})$, respectively.

lated combinations which prefer lower values of H_0 . The inclusion of SS data in the Hu-Sawicki model can partially alleviate the inferred Hubble tension, which is attributed to the modified GW friction term. Quantitatively, the $\text{SS}_{\Lambda\text{CDM}}:\text{PP+CC}$ combination gives a tension of $\sim 0.01\sigma$, while the Planck- and DESI2-based SS simulations yield $\sim 0.41\sigma$ and $\sim 2.44\sigma$ respectively.

Interestingly, as shown in Fig. 1, the $w_{\text{eff}0} - b$ contours from the PP+CC and DESI2 related datasets exhibit a characteristic “butterfly”-like morphology, where $w_{\text{eff}0}$ and b are positively correlated for $b < 0$ but are negatively for $b > 0$. Consistently, Fig. 3 shows that the effective equation-of-state parameter $w_{\text{eff}}(z)$ displays oscillations with redshift. Also, w_{eff} can cross the phantom divide and evolve from

Table 2 Constraints on the derived quantities (F_{R0} , F_{RR0} , r_0 , m_0) and the information criteria (ΔAIC , ΔBIC) for the Hu-Sawicki and Starobinsky models. Since HS:SS $_{\Lambda\text{CDM}}\text{PP+CC}$ is generated using the ΛCDM best-fit fiducial parameters (Ω_{m0} , H_0 , b) = (0.348, 72.99, 0), we also report the corresponding AIC and BIC comparison between HS:SS $_{\Lambda\text{CDM}}\text{PP+CC}$ and $\Lambda\text{CDM:SS}_{\text{PP+CC}}$.

Data	$F_{R0}(10^{-3})$	$F_{RR0}(10^{-7})$	r_0	$m_0(10^{-3})$	ΔAIC	ΔBIC
HS:PP+CC	$-47.72^{+14.21+47.45}_{-26.10-41.00}$	$12.75^{+4.15+4.71}_{-0.42-11.49}$	$-1.602^{+0.104+0.166}_{-0.055-0.182}$	$86.01^{+48.78+62.60}_{-16.09-80.55}$	-0.8	4.7
HS:SS $_{\Lambda\text{CDM}}\text{PP+CC}$	$-12.00^{+17.82+56.03}_{-37.58-47.58}$	$3.51^{+14.49+15.64}_{-59.29-23.45}$	$-1.726^{+0.156+0.203}_{-0.077-0.244}$	$21.32^{+71.12+88.35}_{-10.89-67.87}$	2.5	7.4
HS:PP+CC+SS $_{\Lambda\text{CDM}}\text{PP+CC}$	$-16.62^{+14.18+50.51}_{-29.22-39.39}$	$5.30^{+0.30+12.46}_{-2.94-6.89}$	$-1.716^{+0.130+0.155}_{-0.046-0.218}$	$30.80^{+56.21+73.29}_{-38.72-38.24}$	2.4	8.3
HS: Planck	$10.46^{+1.30+215.33}_{-84.51-96.43}$	$-13.53^{+41.79+45.24}_{-10.09-130.32}$	$-1.955^{+0.422+67.129}_{-0.219-28.968}$	$-32.53^{+163.31+174.86}_{-19.69-467.53}$	3.9	3.0
HS:SS $_{\text{Planck}}$	$4.35^{+16.93+125.93}_{-60.57-77.75}$	$-8.35^{+29.39+32.58}_{-0.36-98.91}$	$-1.830^{+0.267+0.338}_{-0.065-0.570}$	$-14.56^{+121.36+148.31}_{-23.75-265.68}$	—	—
HS: Planck+SS $_{\text{Planck}}$	$-21.46^{+7.04+15.86}_{-8.49-15.38}$	$9.40^{+3.66+6.22}_{-2.73-9.04}$	$-1.714^{+0.044+0.078}_{-0.035-0.080}$	$41.45^{+16.30+28.19}_{-12.73-39.76}$	—	—
HS:DESI2	$-4.24^{+14.59+46.88}_{-27.24-39.00}$	$1.31^{+12.22+16.53}_{-5.32-21.51}$	$-1.805^{+0.134+0.190}_{-0.068-0.228}$	$7.15^{+54.69+75.27}_{-26.13-94.49}$	2.9	3.4
HS:SS $_{\text{DESI2}}$	$-43.90^{+14.23+20.44}_{-41.74-54.21}$	$10.95^{+8.24+9.28}_{-1.96-25.33}$	$-1.628^{+0.175+0.235}_{-0.066-0.312}$	$76.78^{+77.62+81.20}_{-9.39-132.6}$	—	—
HS:DESI2+SS $_{\text{DESI2}}$	$-11.64^{+11.73+19.53}_{-10.90-18.28}$	$4.87^{+4.77+7.39}_{-3.02-8.21}$	$-1.767^{+0.053+0.089}_{-0.039-0.094}$	$22.67^{+21.81+35.13}_{-22.80-38.08}$	—	—
StarI:PP+CC	$-0.92^{+0.28+0.57}_{-0.28-0.56}$	$0.57^{+0.18+0.40}_{-0.21-0.39}$	$-1.824^{+0.031+0.032}_{-0.022-0.028}$	$2.77^{+0.84+1.67}_{-0.84-1.72}$	-2.4	3.1
StarII:PP+CC	$-0.92^{+0.28+0.60}_{-0.28-0.56}$	$0.57^{+0.19+0.40}_{-0.21-0.41}$	$-1.825^{+0.032+0.055}_{-0.022-0.059}$	$2.76^{+0.85+1.68}_{-0.91-1.79}$	-2.4	3.1
StarI:SS $_{\text{PP+CC}}$	$-1.01^{+0.35+0.43}_{-0.07-0.75}$	$0.67^{+0.02+0.73}_{-0.32-0.37}$	$-1.816^{+0.010+0.063}_{-0.031-0.040}$	$3.04^{+0.20+2.24}_{-1.06-1.31}$	—	—
StarII:SS $_{\text{PP+CC}}$	$-1.01^{+0.27+0.40}_{-0.11-0.52}$	$0.64^{+0.06+0.47}_{-0.23-0.32}$	$-1.815^{+0.012+0.045}_{-0.023-0.037}$	$3.02^{+0.33+0.15}_{-0.79-1.19}$	—	—
StarI:PP+CC+SS $_{\text{PP+CC}}$	$-0.92^{+0.12+0.22}_{-0.09-0.21}$	$0.56^{+0.07+1.6}_{-0.08-0.16}$	$-1.823^{+0.010+0.021}_{-0.010-0.020}$	$2.75^{+0.29+0.64}_{-0.34-0.65}$	—	—
StarII:PP+CC+SS $_{\text{PP+CC}}$	$-0.97^{+0.10+0.20}_{-0.10-0.22}$	$0.60^{+0.07+0.17}_{-0.08-0.15}$	$-1.817^{+0.010+0.019}_{-0.010-0.020}$	$2.92^{+0.32+0.66}_{-0.32-0.62}$	—	—
StarI: Planck	$-0.95^{+0.02+0.03}_{-0.01-0.03}$	$0.66^{+0.01+0.03}_{-0.01-0.02}$	$-1.819^{+0.001+0.002}_{-0.002-0.003}$	$2.84^{+0.04+0.08}_{-0.04-0.07}$	1.7	0.8
StarII: Planck	$-0.95^{+0.02+0.03}_{-0.01-0.03}$	$0.66^{+0.01+0.03}_{-0.01-0.02}$	$-1.819^{+0.001+0.002}_{-0.002-0.003}$	$2.84^{+0.04+0.08}_{-0.04-0.07}$	1.7	0.8
StarI:SS $_{\text{Planck}}$	$-1.26^{+0.33+0.47}_{-0.07-0.85}$	$1.01^{+0.02+1.04}_{-0.37-0.49}$	$-1.794^{+0.008+0.063}_{-0.026-0.039}$	$3.79^{+0.20+2.53}_{-1.00-1.42}$	—	—
StarII:SS $_{\text{Planck}}$	$-1.12^{+0.29+0.46}_{-0.01-1.31}$	$0.87^{+0.05+1.68}_{-0.32-0.46}$	$-1.806^{+0.004+0.093}_{-0.024-0.041}$	$3.36^{+0.04+3.90}_{-0.87-1.37}$	—	—
StarI: Planck+SS $_{\text{Planck}}$	$-0.95^{+0.02+0.02}_{-0.01-0.02}$	$0.66^{+0.01+0.03}_{-0.01-0.02}$	$-1.820^{+0.001+0.001}_{-0.001-0.001}$	$2.84^{+0.03+0.07}_{-0.04-0.06}$	—	—
StarII: Planck+SS $_{\text{Planck}}$	$-0.94^{+0.01+0.02}_{-0.02-0.03}$	$0.66^{+0.01+0.02}_{-0.01-0.02}$	$-1.820^{+0.001+0.003}_{-0.001-0.002}$	$2.83^{+0.04+0.08}_{-0.04-0.07}$	—	—
StarI:DESI2	$-1.15^{+0.32+0.32}_{-0.13-0.39}$	$0.94^{+0.15+0.51}_{-0.36-0.40}$	$-1.802^{+0.013+0.032}_{-0.022-0.028}$	$3.45^{+0.40+1.16}_{-0.80-0.97}$	-0.4	0.1
StarII:DESI2	$-1.15^{+0.27+0.32}_{-0.13-0.39}$	$0.94^{+0.15+0.51}_{-0.36-0.40}$	$-1.802^{+0.013+0.032}_{-0.022-0.028}$	$3.45^{+0.40+1.16}_{-0.80-0.97}$	-0.4	0.1
StarI:SS $_{\text{DESI2}}$	$-1.24^{+0.10+0.25}_{-0.14-0.27}$	$0.99^{+0.12+0.26}_{-0.12-0.24}$	$-1.794^{+0.011+0.022}_{-0.008-0.021}$	$3.72^{+0.40+0.82}_{-0.31-0.77}$	—	—
StarII:SS $_{\text{DESI2}}$	$-1.47^{+0.33+0.46}_{-0.19-0.58}$	$1.30^{+0.19+0.72}_{-0.42-0.55}$	$-1.777^{+0.017+0.043}_{-0.024-0.035}$	$4.42^{+0.57+1.73}_{-1.01-1.39}$	—	—
StarI:DESI2+SS $_{\text{DESI2}}$	$-1.22^{+0.18+0.27}_{-0.12-0.32}$	$1.01^{+0.12+0.37}_{-0.21-0.31}$	$-1.796^{+0.011+0.026}_{-0.014-0.023}$	$3.67^{+0.34+0.95}_{-0.54-0.83}$	—	—
StarII:DESI2+SS $_{\text{DESI2}}$	$-1.28^{+0.16+0.28}_{-0.13-0.32}$	$1.10^{+0.15+0.40}_{-0.21-0.30}$	$-1.791^{+0.011+0.025}_{-0.013-0.023}$	$3.84^{+0.40+0.97}_{-0.50-0.83}$	—	—

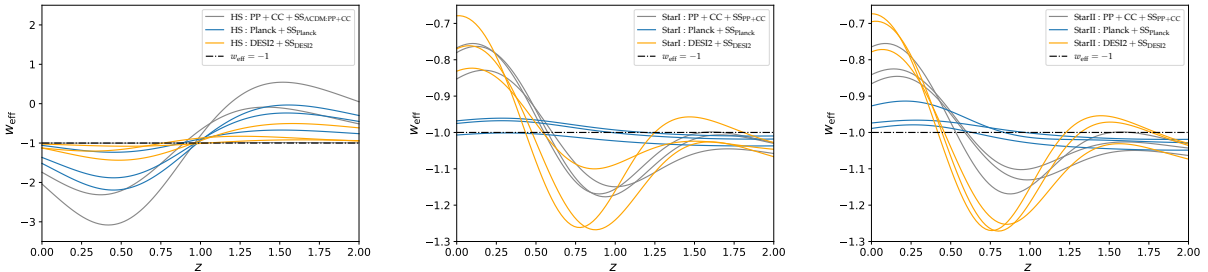


Fig. 3 The evolutions of w_{eff} for the Hu-Sawicki (left), StarobinskyI (middle) and StarobinskyII (right) models, which are based on the the 1σ regimes of PP+CC+SS $_{\Lambda\text{CDM}}\text{PP+CC}$ /PP+CC+SS $_{\text{PP+CC}}$, DESI2+SS $_{\text{DESI2}}$ and Planck+SS $_{\text{Planck}}$ constraining results.

$w_{\text{eff}} < -1$ to $w_{\text{eff}} > -1$ at the redshift range $0 < z < 2$, which may be associated with ghost-like instabilities in the effective description.

For EM-only constraints, only PP+CC excludes $b = 0$ (equivalently $w_{\text{eff}0} = -1$ and $m_0 = 0$) at the 1σ level, and excludes $F_{R0} = 0$ (equivalently $F_{RR0} = 0$ and $r_0 = -2$) at the 2σ level. For the SS simulations, only SS $_{\text{DESI2}}$ yields a departure from ΛCDM comparable to that obtained from

PP+CC. The Planck constraints give a very narrow range of Ω_{m0} , and the $\Omega_{m0} - b$ and $H_0 - b$ contours show no significant correlation. In addition, for Planck-related combinations $w_{\text{eff}0}$ is relatively insensitive to b , leading to a broader allowed range than in the other two cases. After combining Planck with SS $_{\text{Planck}}$, we find that $w_{\text{eff}0} = -1$ is excluded at 1σ , while $b = 0$ (together with $F_{R0} = 0$, $F_{RR0} = 0$, $r_0 = -2$, and $m_0 = 0$) is excluded at 2σ . Notably, except for

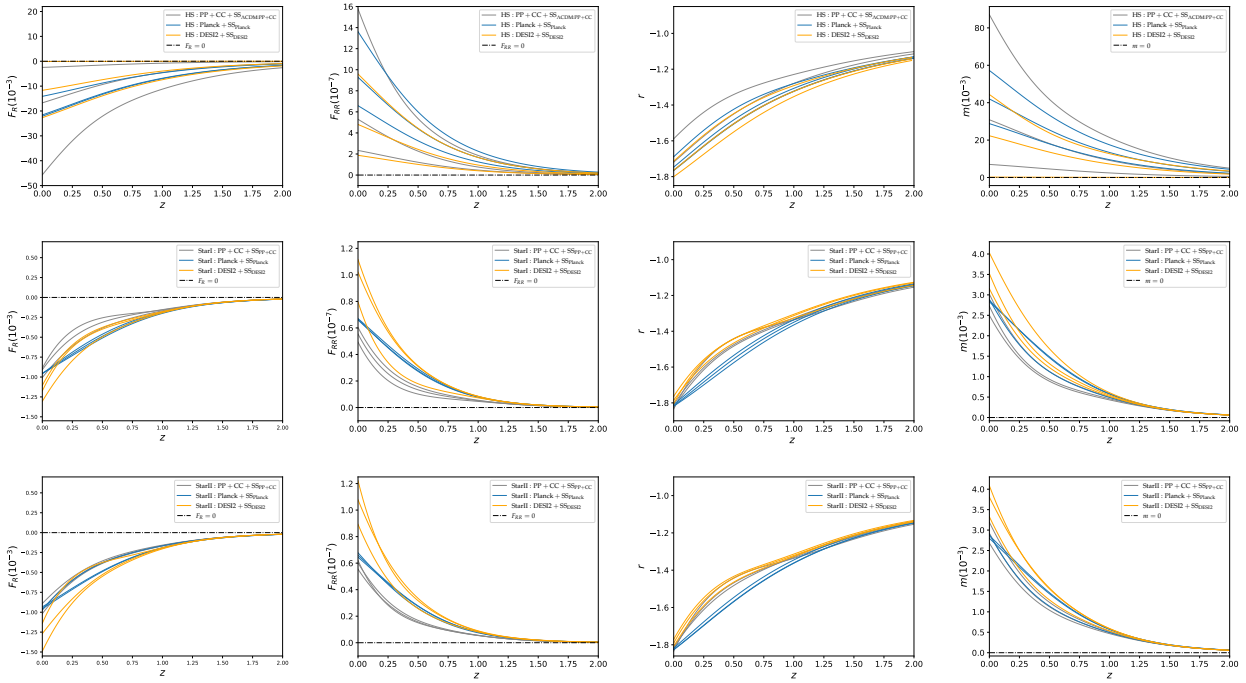


Fig. 4 The evolutions of F_R , F_{RR} , r , and m for the Hu-Sawicki (upper), StarobinskyI (middle) and StarobinskyII (bottom) models, which are based on the the 1σ regimes of $\text{PP+CC+SS}_{\Lambda\text{CDM}}\text{:PP+CC/PP+CC+SS}_{\text{PP+CC}}$, $\text{DESI2+SS}_{\text{DESI2}}$ and $\text{Planck+SS}_{\text{Planck}}$ constraining results.

PP+CC , SS_{DESI2} , and $\text{Planck+SS}_{\text{Planck}}$, the remaining constraints tend to prefer negative values of F_{RR0} , which would imply theoretical instabilities.

Taking into account the preference for negative F_{RR0} , the crossing of $w_{\text{eff}} = -1$, and the BIC results, we conclude that the Hu-Sawicki model may be disfavored and potentially ruled out by future high-precision standard siren data.

4.2 Discussion: Starobinsky model

Since the Starobinsky model is an even function of the deviation parameter b , we impose the prior $b \neq 0$. This choice artificially splits the parameter space into two symmetric branches, $b < 0$ and $b > 0$, which we denote as StarobinskyI and StarobinskyII, respectively. As shown in Table 1, the best-fit χ^2 values of the Starobinsky model are smaller than those of ΛCDM for all datasets. In terms of model selection, only the PP+CC dataset yields $\Delta\text{BIC} = 3.1$, corresponding to weak positive evidence against ΛCDM . For the remaining datasets, the information criteria do not provide decisive discrimination, indicating that ΛCDM and the Starobinsky model are statistically comparable.

The PP+CC -related combinations systematically favor higher values of H_0 than the Planck and DESI2 related combinations, thereby leading to a reduced Hubble tension, similar to the other considered models. Relative to the 5.87σ tension obtained from Planck alone in the StarobinskyI and StarobinskyII branches, adding $\text{SS}_{\text{Planck}}$ mildly alleviates the

tension to $4.70\sigma/4.73\sigma$. In contrast, for PP+CC and DESI2, the inclusion of SS data tends to increase the inferred tension in the Starobinsky model. For instance, in the StarobinskyI model, the $\text{SS}_{\text{PP+CC}}$ and SS_{DESI2} datasets yield tensions of approximately 0.55σ and 9.07σ respectively, whereas the corresponding EM datasets PP+CC/DESI2 give $\sim 0.11\sigma$ and 1.88σ tensions, respectively.

Owing to the imposed prior $b \neq 0$, the posterior distributions for the Planck-related combinations do not always exhibit Gaussian shapes (see Fig. 2). In particular, the SS_{DESI2} posterior in StarobinskyI shows a clear non-Gaussian feature as well. Nevertheless, for EM-only constraints the two branches remain approximately mirror symmetric, again reflecting the evenness of the model. The Ω_{m0} - H_0 contours inferred from PP+CC , Planck, and DESI2 are clearly separated, indicating substantial inconsistencies among the EM datasets. Meanwhile, the SS simulations produce nearly parallel confidence contours, although the sizes of the allowed regions vary. Among the SS cases, the overall constraining power (as inferred from contour areas) follows

$$\text{SS}_{\text{DESI2}} < \text{SS}_{\text{PP+CC}} \leq \text{SS}_{\text{Planck}}.$$

Compared with EM only constraints, adding SS data systematically shifts Ω_{m0} to larger values and H_0 to smaller values. Despite the fact that the SS simulations are generated using symmetric EM best-fit values, the resulting SS constraints are not perfectly symmetric where the StarobinskyI branch typically exhibits a larger deviation from ΛCDM than StarobinskyII for the same $|b|$. This suggests that stan-

dard siren observables are sensitive to the detailed curvature dependence of the $f(R)$ function. Although the Starobinsky model is even in b , cosmological evolution probes only the $R > 0$ branch. And the background dynamics depend nonlinearly on F_R and F_{RR} . For the same $|b|$, the $b < 0$ branch typically approaches the late-time de Sitter attractor more slowly, which can lead to a larger accumulated deviation in the luminosity distance measured by standard sirens.

The $\Omega_{m0} - b$ correlation further illustrates the potential of the Starobinsky model to break parameter degeneracies in a data dependent manner. Specifically, Planck and DESI2 related constraints show a negative correlation, whereas PP+CC favors a positive correlation; the SS constraints also tend to prefer a negative correlation. Although PP+CC alone provides the loosest bounds, its combination with SS data becomes significantly tighter which demonstrates the degeneracy breaking power of standard sirens within this model.

The parameter correlations in the $\Omega_{m0} - b$, $H_0 - b$, and $w_{\text{eff}0} - b$ planes shift signs between StarobinskyI and StarobinskyII because of the mirror symmetry. In particular, $w_{\text{eff}0}$ and b are negatively correlated for $b < 0$, but positively correlated for $b > 0$, producing a “butterfly”-like structure analogous to that found in the Hu-Sawicki case. At the same time, $w_{\text{eff}}(z)$ evolves from the quintessence regime to the phantom regime which is a stable behavior. Notably, the DESI2-related combinations can exclude the Λ CDM limit $b = 0$ (equivalently $w_{\text{eff}0} = -1$) at the 2σ level, providing evidence for dynamical dark energy within the Starobinsky framework. For the Starobinsky model, we constrain F_{R0} at the level of $\mathcal{O}(10^{-3})$, tighter than that in the Hu-Sawicki model (typically $\mathcal{O}(10^{-2})$), and we obtain $F_{RR0} \sim \mathcal{O}(10^{-7})$, which is positive and also smaller than the Hu-Sawicki case (typically $\mathcal{O}(10^{-6})$). Moreover, all data combinations exclude $F_{R0} = 0$, $F_{RR0} = 0$, $r_0 = -2$, and $m_0 = 0$ at the 2σ level for the Starobinsky model. We find that the redshift evolution of w_{eff} in the combined DESI2 data, together with the trajectories of (F_R, F_{RR}, r, m) , can clearly distinguish the Starobinsky scenario from Λ CDM model.

5 Conclusion

In this work, we first constrained the Hu-Sawicki and Starobinsky $f(R)$ models with electromagnetic datasets (PP+CC, Planck, and DESI2) and then simulated standard siren catalogs based on the constrained results. Both $f(R)$ scenarios provide global fits comparable to Λ CDM, and the combined EM+SS analyses yield the tightest constraints.

The simulated SS data offer complementary sensitivity via the modified GW friction term, thereby enhancing the ability to discriminate $f(R)$ gravity from Λ CDM. However, in our simulation-based setup, the inferred Hubble tension is largely dominated by the assumed SS fiducial cosmology. Consequently, while standard sirens can help distin-

guish modified gravity from Λ CDM, they do not provide a viable solution to the Hubble tension in this context.

For the Hu-Sawicki model, SS data can mildly reduce the tension, but several data combinations prefer $F_{RR0} < 0$, suggesting potential theoretical instabilities. We conclude that the Hu-Sawicki model may be disfavored and potentially ruled out by future high-precision standard siren data. For the Starobinsky model, EM-only constraints are nearly symmetric between the $b < 0$ and $b > 0$ branches, whereas SS constraints show mild asymmetries, indicating sensitivity to the curvature dependence of $f(R)$. The redshift evolution of w_{eff} in the combined DESI2 dataset, together with the trajectories of (F_R, F_{RR}, r, m) , clearly distinguishes the Starobinsky scenario from the Λ CDM model. Given the current inconsistencies in the data, future standard siren observations will be essential for a definitive assessment of $f(R)$ gravity as an alternative to the standard cosmological paradigm.

6 Acknowledgements

YZ is supported by National Natural Science Foundation of China under Grant No.12275037 and 12275106. DZH is supported by the Talent Introduction Program of Chongqing University of Posts and Telecommunications (Grant No.E012A2021209), the Youth Science and technology research project of Chongqing Education Committee (Grant No.KJQN202300609).

References

1. **DESI** Collaboration, M. Abdul Karim *et al.*, “DESI DR2 Results II: Measurements of Baryon Acoustic Oscillations and Cosmological Constraints,” [arXiv:2503.14738](https://arxiv.org/abs/2503.14738) [astro-ph.CO].
2. **DESI** Collaboration, K. Lodha *et al.*, “Extended Dark Energy analysis using DESI DR2 BAO measurements,” [arXiv:2503.14743](https://arxiv.org/abs/2503.14743) [astro-ph.CO].
3. E. Di Valentino *et al.*, “Snowmass2021 - Letter of interest cosmology intertwined II: The hubble constant tension,” *Astropart. Phys.* **131** (2021) 102605, [arXiv:2008.11284](https://arxiv.org/abs/2008.11284) [astro-ph.CO].
4. E. Abdalla *et al.*, “Cosmology intertwined: A review of the particle physics, astrophysics, and cosmology associated with the cosmological tensions and anomalies,” *JHEAp* **34** (2022) 49–211, [arXiv:2203.06142](https://arxiv.org/abs/2203.06142) [astro-ph.CO].
5. **Planck** Collaboration, N. Aghanim *et al.*, “Planck 2018 results. VI. Cosmological parameters,” *Astron. Astrophys.* **641** (2020) A6, [arXiv:1807.06209](https://arxiv.org/abs/1807.06209) [astro-ph.CO]. [Erratum: *Astron. Astrophys.* **652**, C4 (2021)].

6. A. G. Riess *et al.*, “A Comprehensive Measurement of the Local Value of the Hubble Constant with $1 \text{ km s}^{-1} \text{ Mpc}^{-1}$ Uncertainty from the Hubble Space Telescope and the SH0ES Team,” *Astrophys. J. Lett.* **934** no. 1, (2022) L7, [arXiv:2112.04510 \[astro-ph.CO\]](#).
7. L. Breuval, A. G. Riess, S. Casertano, W. Yuan, L. M. Macri, M. Romaniello, Y. S. Murakami, D. Scolnic, G. S. Anand, and I. Soszyński, “Small Magellanic Cloud Cepheids Observed with the Hubble Space Telescope Provide a New Anchor for the SH0ES Distance Ladder,” *Astrophys. J.* **973** no. 1, (2024) 30, [arXiv:2404.08038 \[astro-ph.CO\]](#).
8. Y. S. Murakami, A. G. Riess, B. E. Stahl, W. D. Kenworthy, D.-M. A. Pluck, A. Macorett, D. Brout, D. O. Jones, D. M. Scolnic, and A. V. Filippenko, “Leveraging SN Ia spectroscopic similarity to improve the measurement of H_0 ,” *JCAP* **11** (2023) 046, [arXiv:2306.00070 \[astro-ph.CO\]](#).
9. R. C. Nunes, S. Pan, E. N. Saridakis, and E. M. C. Abreu, “New observational constraints on $f(R)$ gravity from cosmic chronometers,” *JCAP* **01** (2017) 005, [arXiv:1610.07518 \[astro-ph.CO\]](#).
10. C. R. Farrugia, J. Sultana, and J. Mifsud, “Spatial curvature in $f(R)$ gravity,” *Phys. Rev. D* **104** no. 12, (2021) 123503, [arXiv:2106.04657 \[astro-ph.CO\]](#).
11. R. D’Agostino and R. C. Nunes, “Measurements of H_0 in modified gravity theories: The role of lensed quasars in the late-time Universe,” *Phys. Rev. D* **101** no. 10, (2020) 103505, [arXiv:2002.06381 \[astro-ph.CO\]](#).
12. S. Basilakos, S. Nesseris, and L. Perivolaropoulos, “Observational constraints on viable $f(R)$ parametrizations with geometrical and dynamical probes,” *Phys. Rev. D* **87** no. 12, (2013) 123529, [arXiv:1302.6051 \[astro-ph.CO\]](#).
13. I. S. Matos, M. O. Calvão, and I. Waga, “Gravitational wave propagation in $f(R)$ models: New parametrizations and observational constraints,” *Phys. Rev. D* **103** no. 10, (2021) 104059, [arXiv:2104.10305 \[gr-qc\]](#).
14. M. Leizerovich, L. Krasilburd, S. J. Landau, and C. G. Scóccola, “Testing $f(R)$ gravity models with quasar x-ray and UV fluxes,” *Phys. Rev. D* **105** no. 10, (2022) 103526, [arXiv:2112.01492 \[astro-ph.CO\]](#).
15. P. Bessa, M. Campista, and A. Bernui, “Observational constraints on Starobinsky $f(R)$ cosmology from cosmic expansion and structure growth data,” *Eur. Phys. J. C* **82** (2022) 506, [arXiv:2112.00822 \[astro-ph.CO\]](#).
16. S. Jana and S. Mohanty, “Constraints on $f(R)$ theories of gravity from GW170817,” *Phys. Rev. D* **99** no. 4, (2019) 044056, [arXiv:1807.04060 \[gr-qc\]](#).
17. L. Amendola, R. Gannouji, D. Polarski, and S. Tsujikawa, “Conditions for the cosmological viability of $f(R)$ dark energy models,” *Phys. Rev. D* **75** (2007) 083504, [arXiv:gr-qc/0612180](#).
18. S. Capozziello and S. Tsujikawa, “Solar system and equivalence principle constraints on $f(R)$ gravity by chameleon approach,” *Phys. Rev. D* **77** (2008) 107501, [arXiv:0712.2268 \[gr-qc\]](#).
19. X. Fu, P. Wu, and H. W. Yu, “The growth factor of matter perturbations in $f(R)$ gravity,” *Eur. Phys. J. C* **68** (2010) 271–276, [arXiv:1012.2249 \[gr-qc\]](#).
20. B. Hu, M. Raveri, M. Rizzato, and A. Silvestri, “Testing Hu–Sawicki $f(R)$ gravity with the effective field theory approach,” *Mon. Not. Roy. Astron. Soc.* **459** no. 4, (2016) 3880–3889, [arXiv:1601.07536 \[astro-ph.CO\]](#).
21. L. Amendola, D. Polarski, and S. Tsujikawa, “Are $f(R)$ dark energy models cosmologically viable ?,” *Phys. Rev. Lett.* **98** (2007) 131302, [arXiv:astro-ph/0603703](#).
22. S. D. Odintsov, D. Sáez-Chillón Gómez, and G. S. Sharov, “Analyzing the H_0 tension in $F(R)$ gravity models,” *Nucl. Phys. B* **966** (2021) 115377, [arXiv:2011.03957 \[gr-qc\]](#).
23. D. Kumar, P. K. Dhankar, S. Ray, and F. Zhang, “Joint analysis of constraints on $f(R)$ parametrization from recent cosmological observations,” *Phys. Dark Univ.* **49** (2025) 101989, [arXiv:2504.04118 \[astro-ph.CO\]](#).
24. S. He and W. Yang, “Cosmological analysis of a viable $f(R)$ gravity model,” [arXiv:2601.16641 \[astro-ph.CO\]](#).
25. **LIGO Scientific, Virgo** Collaboration, B. P. Abbott *et al.*, “Observation of Gravitational Waves from a Binary Black Hole Merger,” *Phys. Rev. Lett.* **116** no. 6, (2016) 061102, [arXiv:1602.03837 \[gr-qc\]](#).
26. **LIGO Scientific, Virgo** Collaboration, B. P. Abbott *et al.*, “GW170817: Observation of Gravitational Waves from a Binary Neutron Star Inspiral,” *Phys. Rev. Lett.* **119** no. 16, (2017) 161101, [arXiv:1710.05832 \[gr-qc\]](#).
27. **LIGO Scientific, Virgo, Fermi-GBM, INTEGRAL** Collaboration, B. P. Abbott *et al.*, “Gravitational Waves and Gamma-rays from a Binary Neutron Star Merger: GW170817 and GRB 170817A,” *Astrophys. J. Lett.* **848** no. 2, (2017) L13, [arXiv:1710.05834 \[astro-ph.HE\]](#).
28. **LIGO Scientific, Virgo** Collaboration, B. P. Abbott *et al.*, “GWTC-1: A Gravitational-Wave Transient Catalog of Compact Binary Mergers Observed by LIGO and Virgo during the First and Second Observing Runs,” *Phys. Rev. X* **9** no. 3, (2019) 031040, [arXiv:1811.12907 \[astro-ph.HE\]](#).

29. **LIGO Scientific, Virgo** Collaboration, R. Abbott *et al.*, “GWTC-2: Compact Binary Coalescences Observed by LIGO and Virgo During the First Half of the Third Observing Run,” *Phys. Rev. X* **11** (2021) 021053, arXiv:2010.14527 [gr-qc].

30. **LIGO Scientific, VIRGO, KAGRA** Collaboration, A. G. Abac *et al.*, “GWTC-4.0: Updating the Gravitational-Wave Transient Catalog with Observations from the First Part of the Fourth LIGO-Virgo-KAGRA Observing Run,” arXiv:2508.18082 [gr-qc].

31. E. Belgacem, Y. Dirian, S. Foffa, and M. Maggiore, “Gravitational-wave luminosity distance in modified gravity theories,” *Phys. Rev. D* **97** no. 10, (2018) 104066, arXiv:1712.08108 [astro-ph.CO].

32. **LISA Cosmology Working Group** Collaboration, E. Belgacem *et al.*, “Testing modified gravity at cosmological distances with LISA standard sirens,” *JCAP* **07** (2019) 024, arXiv:1906.01593 [astro-ph.CO].

33. D. E. Holz and S. A. Hughes, “Using gravitational-wave standard sirens,” *Astrophys. J.* **629** (2005) 15–22, arXiv:astro-ph/0504616.

34. B. F. Schutz, “Determining the Hubble Constant from Gravitational Wave Observations,” *Nature* **323** (1986) 310–311.

35. T. G. F. Li, “Extracting physics from gravitational waves: Testing the strong-field dynamics of general relativity and inferring the large-scale structure of the universe,” 2015. <https://api.semanticscholar.org/CorpusID:123983687>.

36. M. Maggiore, *Gravitational Waves. Vol. 1: Theory and Experiments*. Oxford University Press, 2007.

37. W. Zhao, C. Van Den Broeck, D. Baskaran, and T. G. F. Li, “Determination of Dark Energy by the Einstein Telescope: Comparing with CMB, BAO and SNIa Observations,” *Phys. Rev. D* **83** (2011) 023005, arXiv:1009.0206 [astro-ph.CO].

38. R.-G. Cai and T. Yang, “Estimating cosmological parameters by the simulated data of gravitational waves from the Einstein Telescope,” *Phys. Rev. D* **95** no. 4, (2017) 044024, arXiv:1608.08008 [astro-ph.CO].

39. X. Su, D. He, and Y. Zhang, “The Einstein Telescope standard siren simulations for $f(Q)$ cosmologies,” *Eur. Phys. J. C* **85** no. 3, (2025) 358, arXiv:2408.03725 [gr-qc].

40. Y. Zhang and H. Zhang, “Distinguish the $f(T)$ model from Λ CDM model with Gravitational Wave observations,” *Eur. Phys. J. C* **81** no. 8, (2021) 706, arXiv:2108.05736 [astro-ph.CO].

41. W. Hu and I. Sawicki, “Models of $f(R)$ Cosmic Acceleration that Evade Solar-System Tests,” *Phys. Rev. D* **76** (2007) 064004, arXiv:0705.1158 [astro-ph].

42. A. A. Starobinsky, “Disappearing cosmological constant in $f(R)$ gravity,” *JETP Lett.* **86** (2007) 157–163, arXiv:0706.2041 [astro-ph].

43. R. D’Agostino and R. C. Nunes, “Probing observational bounds on scalar-tensor theories from standard sirens,” *Phys. Rev. D* **100** no. 4, (2019) 044041, arXiv:1907.05516 [gr-qc].

44. S. Tsujikawa, “Observational signatures of $f(R)$ dark energy models that satisfy cosmological and local gravity constraints,” *Phys. Rev. D* **77** (2008) 023507, arXiv:0709.1391 [astro-ph].

45. L. Yang, C.-C. Lee, and C.-Q. Geng, “Gravitational Waves in Viable $f(R)$ Models,” *JCAP* **08** (2011) 029, arXiv:1106.5582 [astro-ph.CO].

46. A. Lewis and S. Bridle, “Cosmological parameters from CMB and other data: A Monte Carlo approach,” *Phys. Rev. D* **66** (2002) 103511, arXiv:astro-ph/0205436.

47. M. Moresco, R. Jimenez, L. Verde, A. Cimatti, and L. Pozzetti, “Setting the Stage for Cosmic Chronometers. II. Impact of Stellar Population Synthesis Models Systematics and Full Covariance Matrix,” *Astrophys. J.* **898** no. 1, (2020) 82, arXiv:2003.07362 [astro-ph.GA].

48. A. Favale, A. Gómez-Valent, and M. Migliaccio, “Cosmic chronometers to calibrate the ladders and measure the curvature of the Universe. A model-independent study,” *Mon. Not. Roy. Astron. Soc.* **523** no. 3, (2023) 3406–3422, arXiv:2301.09591 [astro-ph.CO].

49. D. Scolnic *et al.*, “The Pantheon+ Analysis: The Full Data Set and Light-curve Release,” *Astrophys. J.* **938** no. 2, (2022) 113, arXiv:2112.03863 [astro-ph.CO].

50. D. Brout *et al.*, “The Pantheon+ Analysis: Cosmological Constraints,” *Astrophys. J.* **938** no. 2, (2022) 110, arXiv:2202.04077 [astro-ph.CO].

51. C. Zhang, H. Zhang, S. Yuan, T.-J. Zhang, and Y.-C. Sun, “Four new observational $H(z)$ data from luminous red galaxies in the Sloan Digital Sky Survey data release seven,” *Res. Astron. Astrophys.* **14** no. 10, (2014) 1221–1233, arXiv:1207.4541 [astro-ph.CO].

52. R. Jimenez, L. Verde, T. Treu, and D. Stern, “Constraints on the equation of state of dark energy and the Hubble constant from stellar ages and the CMB,” *Astrophys. J.* **593** (2003) 622–629, arXiv:astro-ph/0302560.

53. M. Moresco, L. Verde, L. Pozzetti, R. Jimenez, and A. Cimatti, “New constraints on cosmological parameters and neutrino properties using the expansion rate of the Universe to $z \sim 1.75$,” *JCAP* **07** (2012) 053, [arXiv:1201.6658 \[astro-ph.CO\]](https://arxiv.org/abs/1201.6658).

54. M. Moresco, “Raising the bar: new constraints on the Hubble parameter with cosmic chronometers at $z \sim 2$,” *Mon. Not. Roy. Astron. Soc.* **450** no. 1, (2015) L16–L20, [arXiv:1503.01116 \[astro-ph.CO\]](https://arxiv.org/abs/1503.01116).

55. J. Simon, L. Verde, and R. Jimenez, “Constraints on the redshift dependence of the dark energy potential,” *Phys. Rev. D* **71** (2005) 123001, [arXiv:astro-ph/0412269](https://arxiv.org/abs/astro-ph/0412269).

56. C.-H. Chuang and Y. Wang, “Measurements of $H(z)$ and $D_A(z)$ from the Two-Dimensional Two-Point Correlation Function of Sloan Digital Sky Survey Luminous Red Galaxies,” *Mon. Not. Roy. Astron. Soc.* **426** (2012) 226, [arXiv:1102.2251 \[astro-ph.CO\]](https://arxiv.org/abs/1102.2251).

57. M. Moresco, L. Pozzetti, A. Cimatti, R. Jimenez, C. Maraston, L. Verde, D. Thomas, A. Citro, R. Tojeiro, and D. Wilkinson, “A 6% measurement of the Hubble parameter at $z \sim 0.45$: direct evidence of the epoch of cosmic re-acceleration,” *JCAP* **05** (2016) 014, [arXiv:1601.01701 \[astro-ph.CO\]](https://arxiv.org/abs/1601.01701).

58. D. Stern, R. Jimenez, L. Verde, M. Kamionkowski, and S. A. Stanford, “Cosmic Chronometers: Constraining the Equation of State of Dark Energy. I: $H(z)$ Measurements,” *JCAP* **02** (2010) 008, [arXiv:0907.3149 \[astro-ph.CO\]](https://arxiv.org/abs/0907.3149).

59. N. Borghi, M. Moresco, and A. Cimatti, “Toward a Better Understanding of Cosmic Chronometers: A New Measurement of $H(z)$ at $z \sim 0.7$,” *Astrophys. J. Lett.* **928** no. 1, (2022) L4, [arXiv:2110.04304 \[astro-ph.CO\]](https://arxiv.org/abs/2110.04304).

60. A. E. Sasi and M. V. John, “Evolution of Hubble parameter from Pantheon+ data and comparison of cosmological models using cosmic chronometers,” 12, 2024. [arXiv:2412.14184 \[astro-ph.CO\]](https://arxiv.org/abs/2412.14184).

61. A. Gómez-Valent and L. Amendola, “ H_0 from cosmic chronometers and Type Ia supernovae, with Gaussian Processes and the novel Weighted Polynomial Regression method,” *JCAP* **04** (2018) 051, [arXiv:1802.01505 \[astro-ph.CO\]](https://arxiv.org/abs/1802.01505).

62. W. Hu and N. Sugiyama, “Small scale cosmological perturbations: An Analytic approach,” *Astrophys. J.* **471** (1996) 542–570, [arXiv:astro-ph/9510117](https://arxiv.org/abs/astro-ph/9510117).

63. G. Efstathiou and J. R. Bond, “Cosmic confusion: Degeneracies among cosmological parameters derived from measurements of microwave background anisotropies,” *Mon. Not. Roy. Astron. Soc.* **304** (1999) 75–97, [arXiv:astro-ph/9807103](https://arxiv.org/abs/astro-ph/9807103).

64. Y. Wang and P. Mukherjee, “Robust dark energy constraints from supernovae, galaxy clustering, and three-year wilkinson microwave anisotropy probe observations,” *Astrophys. J.* **650** (2006) 1–6, [arXiv:astro-ph/0604051](https://arxiv.org/abs/astro-ph/0604051).

65. Y. Wang and P. Mukherjee, “Observational Constraints on Dark Energy and Cosmic Curvature,” *Phys. Rev. D* **76** (2007) 103533, [arXiv:astro-ph/0703780](https://arxiv.org/abs/astro-ph/0703780).

66. L. Chen, Q.-G. Huang, and K. Wang, “Distance Priors from Planck Final Release,” *JCAP* **02** (2019) 028, [arXiv:1808.05724 \[astro-ph.CO\]](https://arxiv.org/abs/1808.05724).

67. Z. Zhai, C.-G. Park, Y. Wang, and B. Ratra, “CMB distance priors revisited: effects of dark energy dynamics, spatial curvature, primordial power spectrum, and neutrino parameters,” *JCAP* **07** (2020) 009, [arXiv:1912.04921 \[astro-ph.CO\]](https://arxiv.org/abs/1912.04921).

68. Z. Zhai and Y. Wang, “Robust and model-independent cosmological constraints from distance measurements,” *JCAP* **07** (2019) 005, [arXiv:1811.07425 \[astro-ph.CO\]](https://arxiv.org/abs/1811.07425).

69. C. Hahn *et al.*, “The DESI Bright Galaxy Survey: Final Target Selection, Design, and Validation,” *Astron. J.* **165** no. 6, (2023) 253, [arXiv:2208.08512 \[astro-ph.CO\]](https://arxiv.org/abs/2208.08512).

70. **DESI** Collaboration, R. Zhou *et al.*, “Target Selection and Validation of DESI Luminous Red Galaxies,” *Astron. J.* **165** no. 2, (2023) 58, [arXiv:2208.08515 \[astro-ph.CO\]](https://arxiv.org/abs/2208.08515).

71. A. Raichoor *et al.*, “Target Selection and Validation of DESI Emission Line Galaxies,” *Astron. J.* **165** no. 3, (2023) 126, [arXiv:2208.08513 \[astro-ph.CO\]](https://arxiv.org/abs/2208.08513).

72. E. Chaussidon *et al.*, “Target Selection and Validation of DESI Quasars,” *Astrophys. J.* **944** no. 1, (2023) 107, [arXiv:2208.08511 \[astro-ph.CO\]](https://arxiv.org/abs/2208.08511).

73. R. J. Cooke, M. Pettini, and C. C. Steidel, “One Percent Determination of the Primordial Deuterium Abundance,” *Astrophys. J.* **855** no. 2, (2018) 102, [arXiv:1710.11129 \[astro-ph.CO\]](https://arxiv.org/abs/1710.11129).

74. J.-X. Li and S. Wang, “A comprehensive numerical study on four categories of holographic dark energy models,” *JCAP* **07** (2025) 047, [arXiv:2412.09064 \[astro-ph.CO\]](https://arxiv.org/abs/2412.09064).

75. J.-c. Hwang and H.-r. Noh, “Gauge ready formulation of the cosmological kinetic theory in generalized gravity theories,” *Phys. Rev. D* **65** (2002) 023512, [arXiv:astro-ph/0102005](https://arxiv.org/abs/astro-ph/0102005).

76. M. Raveri and W. Hu, “Concordance and Discordance in Cosmology,” *Phys. Rev. D* **99** no. 4, (2019) 043506, [arXiv:1806.04649 \[astro-ph.CO\]](https://arxiv.org/abs/1806.04649).